Journal of Neuroinflammation

RESEARCH

Open Access

T cell receptor activation contributes to brain damage after intracerebral hemorrhage in mice

Yuwen Xiu[1], Yingjie Wang[1], Ningning Wang[2], Ning Liu[1,4], Yinghua Jiang[1,4], Mengxuan Shi[1], Di Zhou[1], Thin Yadanar Sein[1], Mitchell D. Kilgore[1], Prasad V. G. Katakam[1,4], Qiang Liu[2], Wei-Na Jin[3], Fu-Dong Shi[2,3], Xiaoying Wang[1,4*] and Aaron S. Dumont[1,4*]

Abstract

Background Our previous studies demonstrated that activated T cells accumulate in perihematomal regions following intracerebral hemorrhage (ICH) and exacerbate hemorrhagic brain injury. In the present study, we aimed to explore the mechanisms underlying brain-infiltrating T cell activation and the associated pathophysiological effects in neurological outcomes following ICH.

Methods We employed standardized collagenase injection-induced and autologous blood injection models of ICH in male C57BL/6J mice. T cell receptor (TCR) activation, immune cell infiltration, and cytokine production were quantified through immunostaining, flow cytometry, and cytokine arrays at 1- and 3-days post-ICH. Brain edema volume was measured at 3 days post-ICH and neurobehavioral assessments were conducted up to 14 days post-ICH. Pharmacological inhibition of TCR activation was achieved using the TCR-specific inhibitor AX-024, administered intraperitoneally at a dosage of 10 mg/kg 1-hour post-ICH.

Results Flow cytometry and immunostaining detected TCR activation of brain-infiltrating T cells. Specific TCR activation inhibitor AX-024 administration markedly reduced TCR activation and the production of pro-inflammatory cytokines in the brain at 1- and 3-days post-ICH. Moreover, AX-024 administration led to a significant reduction in the infiltration of other leukocyte populations, and significantly reduced brain edema while improved long-term sensorimotor and cognitive outcomes up to 14 days post-ICH.

Discussion Our findings underscore the critical role of TCR activation in the mobilization and activation of brain-infiltrating T cells post-ICH. Inhibition of TCR activation via AX-024 administration might be developed as a promising therapeutic strategy to improve neurological outcomes following ICH. However, further research is necessary to thoroughly explore the complex pathophysiological processes involved.

Keywords Intracerebral hemorrhage, Inflammation, T-cell receptor, T cell activation, Leukocyte

*Correspondence:
Xiaoying Wang
xwang51@tulane.edu
Aaron S. Dumont
adumont2@tulane.edu
[1]Clinical Neurosciences Research Center, Department of Neurosurgery, Tulane University School of Medicine, New Orleans, LA, USA
[2]Department of Neurology, Tianjin Medical University General Hospital, Tianjin, China
[3]Center of Neurological Diseases, China National Clinical Research Center for Neurological Diseases, Beijing Tiantan Hospital, Capital Medical University, Beijing, China
[4]Neuroscience Program, Tulane Brain Institute, Tulane University, New Orleans, LA, USA

Background

Intracerebral hemorrhage (ICH) is a severe neurological emergency characterized by abrupt, spontaneous bleeding into the brain parenchyma, resulting in high morbidity and mortality rates [1]. This condition remains a formidable challenge in the clinical setting due to its poor prognosis and the paucity of effective therapeutic strategies [2]. Neuroinflammation is a central detrimental process that occurs following ICH and is initiated by the presence of blood by products in the brain parenchyma. It is characterized by the activation of resident immune cells, including microglia and astrocytes, alongside the infiltration of peripheral immune cells into the brain parenchyma, resulting in the release of pro-inflammatory cytokines, chemokines, and reactive oxygen species. In the acute phase following ICH, these inflammatory mediators contribute to blood-brain barrier (BBB) disruption, neuronal damage, and cerebral edema while promote neuronal apoptosis and impair neuroplasticity, ultimately exacerbate neurological deficits. Understanding the mechanisms and cellular factors involved in this neuroinflammation is essential for developing effective therapies to reduce secondary injury and improve neurological outcomes after ICH [3].

Preclinical investigations have found that T lymphocytes, a predominant population of peripheral leukocytes, are present in the brain up to 14 days after ICH [4, 5]. By using antibody-based T cell depletion methods or blocking T cell egress from peripheral lymphoid tissues with high-affinity sphingosine-1-phosphate receptors (S1PR) agonists such as fingolimod, experimental results from our group and others have shown that the general presence of T cells in the brain during the acute phase of ICH is detrimental [6, 7]. However, considering the neurological outcomes reported in the clinical trial (NCT03338998) and the presence of off-target side effects, the clinical applicability of S1PR agonists for treating ICH remains constrained [8, 9]. Consequently, it is crucial to deepen our understanding of the roles and mechanisms underlying the intricate immunopathology of T lymphocytes following ICH. This knowledge will facilitate the development of targeted therapeutic strategies aimed at mitigating the harmful effects of specific subsets of brain-infiltrating T lymphocytes in this context [10].

Our previously published study revealed an accumulation of brain-infiltrating T lymphocytes in the peri-hematoma regions in both human subjects and murine models during the acute phase of ICH [11]. We found that the depletion of $CD4^+$ T cells reduced perihematomal edema (PHE) volumes and mitigated neurological deficits in murine ICH models [11], demonstrating a detrimental role of acutely infiltrating T cells post-ICH. Interestingly, we found that brain infiltrating T lymphocytes were activated concurrently with the development of PHE, suggesting the T cell activation process might be a critical checkpoint in triggering brain infiltrating T cell-mediated detrimental neuroinflammation in the acute phase after ICH [11]. However, the molecular mechanisms driving the inflammatory activation of brain infiltrating T lymphocytes post-ICH remain unknown.

T cell activation is tightly regulated by T-cell receptor (TCR)-dependent and TCR-independent mechanisms. Upon engagement of the TCR with the major histocompatibility complex (MHC) on antigen-presenting cells (APCs), intracellular signaling is rapidly initiated and leads to the phosphorylation of a series of downstream signaling molecules including ZAP70, a non-catalytic region of tyrosine kinase adaptor protein (NCK), and linker for activation of T cells (LAT) that ultimately results in T cell differentiation [12]. Additionally, T cells can also be activated via TCR-independent mechanisms, including through the CD2 and Toll-like receptor pathways [13, 14]. Although the mechanisms of T cell activation post-ICH need to be further elucidated [15], emerging evidence has indicated that TCR-dependent T cell activation may, in fact, play an important pathological role in the acute phase of brain injury [16, 17].

In this study, we hypothesized that TCR-dependent T cell activation plays a pivotal role in the proinflammatory actions of brain-infiltrating T lymphocytes after ICH, thereby intensifying the neuroinflammatory response. Blocking TCR activation with a specific TCR activation inhibitor might diminish T cell activation, and consequently mitigate acute detrimental neuroinflammation and the associated secondary brain damage, and neurological deficits post-ICH.

Methods

Animals and drug administration

All animal experiments were performed in accordance with the ARRIVE (Animal Research: Reporting In Vivo Experiments) guidelines and approved protocols from the Institutional Animal Care and Use Committee (IACUC) of Tulane University. Three- to four-month-old C57BL/6J (Jackson Laboratory, 000664) male mice were used [18]. Animals were housed under pathogen-free conditions, with standardized light-dark cycles, and free access to food and water. AX-024 (Axon Medchem, 2692, 10 mg/kg) was intraperitoneally (i.p.) administered beginning at 1-hour post-ICH once a day up to 3 days after ICH following the established dose regimen in mice [19]. Vehicle control mice received Phosphate-Buffered Saline (PBS).

ICH models in mice

ICH models were induced by intra-striatal injection of autologous blood or bacterial collagenase as previously described [20]. Briefly, a 1-mm-diameter burr hole was

created on the right side of the skull, 2.3 mm lateral to midline, 0.5 mm anterior to bregma. In the autologous blood model, 30 μL of non-heparinized autologous blood was injected. In the bacterial collagenase injection model, 0.0375U of bacterial collagenase (Type IV-S, Sigma-Aldrich, C4-28) in 0.9 μL of saline was injected at the same coordinates at a rate of 0.5 μL/min. All injections occurred at a depth of 3.7 mm beneath the skull. During the surgery, body temperature was maintained at 37 °C ± 0.5 °C. Following injection, the cranial burr hole was sealed with bone wax, the skin incision was sutured, and the mice were returned to their cages under close observation until fully recovered from anesthesia.

Assessment of neurological deficit

Randomization was applied for group assignments, and investigators were blinded for all animal group assignments, treatments, and endpoints throughout all experiments. Motor function was assessed on day 1,3,7,14 after ICH by modified neurological scale score (mNSS), adhesive removal test, and foot fault test as previously described [21]. The mNSS rates neurological function on a scale of 0–18 points, including motor, sensory, reflex, and balance tests. The higher scores summed, the more severe the deficit is. The adhesive removal test was performed to access the ipsilateral forepaw sensitivity and motor impairments. The results of the time-to-contact and time-to remove were recorded [22]. The result of foot fault test was quantified as percentage of fault steps referring to the total steps as previously described [23]. Before surgery, the animals were trained for 2 days.

Spatial learning and memory were assessed using Morri's water maze (MWM) test on days 10–14 after ICH, as previously described [24]. Mouse water maze tank (diameter: 120 cm) are filled with water, and a round plastic platform (diameter: 10 cm, height: 30 cm) was positioned 1.5 cm below the surface of the water. The water temperature was at 21 ± 1 °C. Mice were trained by seven hidden platforms trails, including one hidden platform trail on day 10 after ICH, and two hidden platform trails/day on day 11–13 after ICH. A probe trial was carried out on day 14 after ICH. For seven hidden platforms trails, mice were placed in the tank facing the wall and allowed up to 90s to locate the platform. For probe trail, mice were placed in the tank without the platform and allowed to swim for 60s to explore the tank. The trajectories were recorded with a video tracking system and analyzed by ANY-maze software (Stoelting Co., Wood Dale. IL).

Immunostaining

Immunostaining was conducted as previously described [25]. Briefly, 8-μm frozen, paraformaldehyde-fixed sections were mounted to glass slides and blocked with 10% donkey serum, 3% bovine serum albumin, and 0.3% Triton X-100 in 1x PBS for 1 h. Primary incubation was performed at 4 °C overnight using the following primary antibodies: phospho-LAT (Tyr161) (Invitrogen, PA5-105929), CD3 (Invitrogen, 14-0032-81), Caspase-1 (p20) (Adipogen, AG-20B-0042), Iba1 (Wako, 019-19741), Myelin Basic Protein (MBP) (Abcam, ab40390), Anti-Neurofilament H Non-Phosphorylated antibody (SMI-32) (Millipore Sigma, NE1022). After washing with cold PBS, brain slices were incubated with fluorescence-conjugated secondary antibodies at room temperature for 1 h. Slides were washed and mounted on antifade medium with DAPI (Vector, H-1200-10). We followed a method for quantification of brain-infiltrating immune cell numbers as we previously described with a slight modification [11]. Briefly, five fields of coronal brain slices (located at -0.46 mm from anterior bregma, the cross-brain slice of the largest cerebral hematoma) were acquired in the peri-hematoma striatum region. The total number of T cell ($CD3^+$) and TCR-activated T cells (CD3 and p-LAT double positive T cell) were counted, averaged, and presented T cell numbers/mm^2. Likewise, the total number of microglia ($CD11b^+$) and caspase-1 positive microglia numbers were quantified, averaged, and reported as microglia numbers/mm^2 [11]. To quantify the demyelination volume, the area of demyelination shown by abnormal MBP staining was measured in consecutive sections of a brain, which were sliced by a fixed distance. The lesion volume was calculated in an automated fashion using ImageJ. All images were captured using the same microscope settings and processed with the same parameters in peri-lesion area, the fluorescent intensity of SMI32 or MBP was quantified using ImageJ. The ratio of SMI-32/MBP fluorescence intensities was calculated, and an increase in this ratio is an indicator of white matter injury. The images were acquired on Nikon Eclipse Ti2 confocal microscope (Nikon) or Zeiss Axio Scan.Z1 whole slide scanner (Zeiss) and analyzed by ImageJ software (National Institutes of Health, Bethesda, MD, USA).

Flow cytometry

At 1- or 3-days post-ICH, single-cell suspensions from the ipsilateral hemisphere and peripheral blood were prepared for flow cytometry as previously described [25, 26]. All antibodies were stained at 4 °C for 30 min following the manufacturer's protocols. For intracellular antigen staining, cells were fixed and permeated using the intracellular fixation and permeabilization buffer set (Biolegend, 426803). For the phosphorylated antibodies and transcription factor staining, transcription buffer set (Biolegend, 424401) and true-phos perm buffer (Biolegend, 425401) were used. The following antibodies were used: CD3 (Invitrogen, 25-0032-82), CD4 (Biolegend, 116021), CD11b (Biolegend, 101206), CD45 (Biolegend, 103112), Ly6G (Biolegend, 127622), F4/80 (Biolegend,

123110), NK1.1 (Biolegend, 108714), CD11b (Biolegend, 101206), phosphor-ZAP70/Syk (Tyr319, Tyr352) (Invitrogen, 12-9006-42), phosphor-CD247 (CD3ζ) (Tyr142) (Invitrogen, 53-2478-42), IL-17 A (Invitrogen, 17-7177-81), CD69 (Biolegend, 104507), IL-1β (Invitrogen, 12-7114-82), IFN-γ (Biolegend, 505810), IL-10 (Biolegend, 505006), Granzyme B (Biolegend, 372206), perforin (Biolegend, 154403). The data were acquired by a BD LSRFortessa™ Cell Analyzer (BD Bioscience, San Jose, CA, USA) and analyzed with FlowJo software (Version 10.9.0, FlowJo, LLC).

Splenic monocyte isolation and culture

Splenic cells were isolated from 3- to 4-month-old mice. In brief, freshly isolated spleens were mechanically dissociated in PBS. Splenocytes were then treated with red blood cell lysis buffer (Biolegend, 420302) to eliminate red blood cells and then filtered through a 40 μm cell strainer. Spleen single cell suspensions were incubated with anti-CD11b magnetic beads (Miltenyi Biotec, 130-097-142), and captured using a magnetic separator. Finally, 5×10^5 cells/mL were cultured in RPMI 1640 with 10% FBS.

T cell isolation and in vitro activation assays

For T cell purification, splenic T cells were obtained from 3-to 4-month-old mice. Splenocytes from 3 mice were pooled together for untouched negative magnetic cell separation (Miltenyi Biotec, 130-095-130) according to the manufacturer's protocol in each independent experiment. For T cell activation, purified T cells were suspended in RPMI 1640 with 10% FBS and cultured at 2×10^6 cells/mL in a 24-well plate. For TCR-dependent activation, MACSibeads (T cell Activation Kit, Miltenyi Biotec, 130-093-627) loaded with biotinylated CD3 and CD28 antibodies were added into T cell suspensions to mimic APCs (2×10^6 particles per 2×10^6 cell). For TCR-independent activation, PMA and ionomycin (1:500 dilution) (Cell Stimulation Cocktail, ThermoFisher Scientific, 00-4970-03) were added into single T cell suspensions. T Cells were incubated in vitro for 24 h.

Real-time quantitative PCR

Real-time quantitative PCR (RT-qPCR) were performed as described previously [27]. Briefly, total RNA from cultured cells were isolated with the miRNeasy micro kit (Qiagen, 217084) according to the manufacturer's manuals. For real-time RT-PCR, cDNA was synthesized from 500ng of total RNA using QuantiTect Reverse Transcription Kit A (Qiagen, 205311). RT-qPCR was performed using TaqMan Fast Advanced Master Mix (Applied Biosystems, 4444963) in a QS3 real-time PCR system (Applied Biosystems). The TaqMan probes used in the study were as follows: *Tnfα* (Mn00443258_M1), *Il1β* (Mm00434228_m1), *Hprt* (Mm01545399_m1). RT-qPCR was carried out in triplicate, and the relative expression of target genes (fold change) was determined using the $2 - \Delta\Delta Ct$ method with normalization to *Hprt* expression.

Cytokine proteome profiler array

Ipsilateral hemispheres were collected at 3 days post-ICH. Brain tissue was homogenized in lysis buffer supplemented with protease inhibitor cocktail on ice. Total protein was quantified by BCA assay (Pierce BCA protein assay kit, Thermo Fisher, 23227). The inflammatory cytokine levels in the ipsilateral hemisphere were analyzed using the Mouse Cytokine Proteome Profiler Array Panel Kit (R&D Systems, ARY006) according to the manufacturer's protocol. Immunospots were recorded on the ChemiDoc MP imaging system (Bio-Rad). ImageJ (National Institutes of Health, Bethesda, MA, USA) was used to quantify and determine spot density.

Brain water content

Brain water content was evaluated by a wet/dry method as described previously [28].

Statistical analysis

The sample were not predetermined by power analyses. Numbers were selected on the basis of our prior studies showing sufficient statistical power using similar techniques and animal models [11]. Statistical analyses were performed using Prism 10 software (GraphPad). Data were presented as means ± standard deviation (SD). Randomization was applied for group assignments, and investigators were blinded for all animal group assignments, treatments, and endpoints throughout all experiments. For each statistical analysis, we examined normality by Shapiro–Wilk Normality test and examined homoscedasticity between groups by Levene's test. For comparisons between two groups, a t-test was utilized, while ANOVA was applied to assess differences among multiple groups followed by Tukey's post hot multiple comparison. If the assumption of normality was violated, nonparametric methods, such as the Mann-Whitney test were employed. Values of $P < 0.05$ were considered as statistically significant.

Results

TCR of brain-infiltrating T cells in the peri-hematoma region is activated at the acute phase after ICH in mice

Flow cytometry detected a significant increase in the phosphorylation of key signaling proteins, ZAP70 and CD3ζ, of brain-infiltrating T cells at 24 h post-ICH (Fig. 1A-C). The TCR activation was further validated in the autologous blood injection-induced ICH mouse model where immunohistochemistry demonstrated an upregulation in LAT phosphorylation (p-LAT), a

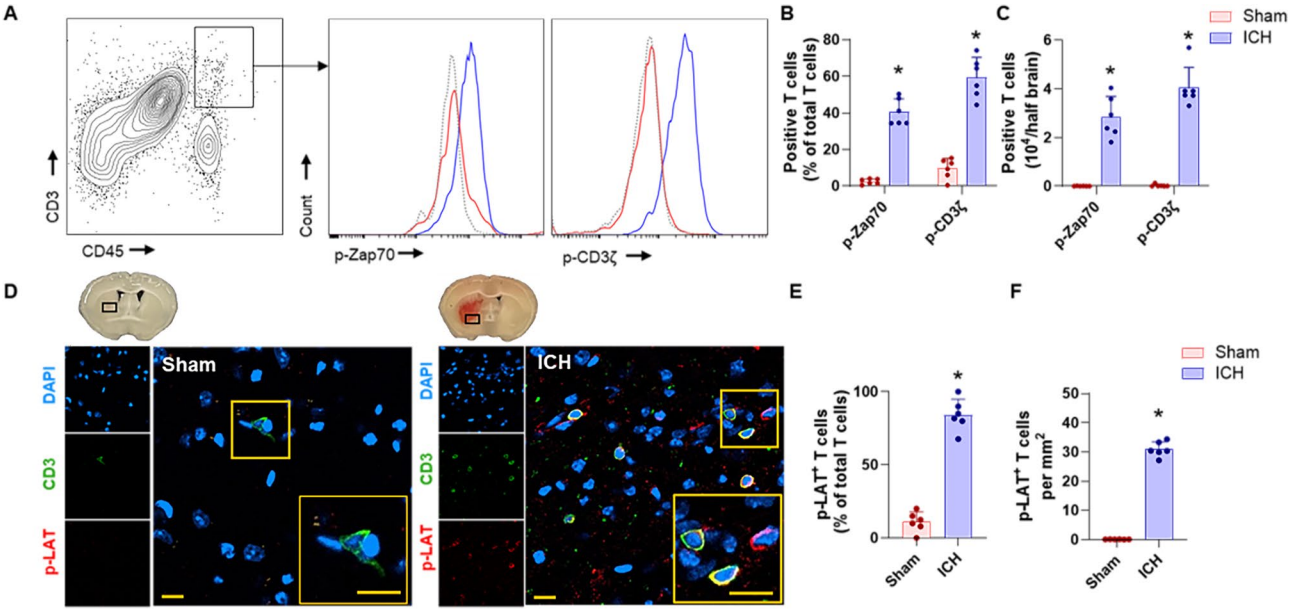

Fig. 1 TCR of brain-infiltrating T cells in the peri-hematoma region is activated at acute phase after ICH in mice. (**A-C**) ICH was induced by injection of collagenase IV in C57BL/6J mice. Brain tissue was harvested at 24 h after ICH. (**A**) Flow cytometry gating to access the expression of phosphorylated Zap70 (p-Zap70) and CD3 ζ (p-CD3ζ) in brain-infiltrating $CD45^+$ $CD3^+$ T cells after ICH. (**B-C**) Comparison of cell counts showing the percentage (**B**) and absolute cell counts (**C**) of p-Zap70 and p-CD3ζ in brain-infiltrating $CD45^+$ $CD3^+$ T cells in sham and ICH groups. $n = 6$ mice per group; Mean ± SD, and $^*P < 0.05$ vs. Sham group. (**D-F**) ICH was induced by injection of autologous blood in C57BL/6J mice. Brain tissue was harvested at 24 h after ICH. (**D**) Double immunostaining of TCR activation marker phosphorylated LAT (p-LAT) with T cells ($CD3^+$) in the peri-hematoma region of both sham and ICH groups. Scale bar: 10 μm. (**E-F**) Comparison of percentage (**E**), and the cell count (**F**) of p-LAT positive T cells in the peri-hematoma area between sham and ICH groups. $n = 6$ mice per group; Mean ± SD, and $^*P < 0.05$ vs. Sham group. $n = 6$ mice per group. Mean ± SD, and $^*P < 0.05$ vs. WT group. Student's t-test in (**B, C, F**) and Mann–Whitney U test in (**E**)

downstream signaling event indicative of TCR activation of T lymphocytes, in the perihematomal region at 24 h post-ICH (Fig. 1D-F). Collectively, these experimental results illustrated the occurrence of acute TCR activation and signaling in brain-infiltrating T cells within the peri-hematoma region following ICH in mice.

Inhibition of TCR activation by AX-024 prevents brain-infiltrating T cell activation at acute phase after ICH in mice

To define the pathological role of TCR activation in the overall activation of brain-infiltrating T lymphocytes during the acute phase of brain injury following ICH, a TCR activation-specific inhibitor AX-024 (10 mg/kg, i.p.) was administered at 1-hour post-ICH. Immunostaining detected a reduction of LAT phosphorylation in the brain-infiltrating T cells at 24 h post-ICH compared to vehicle-treated controls (Fig. 2A-C). Notably, T cells in sham control group were rarely detectable by the immunostaining (data not shown). Whether AX-024 affect p-Zap70 was not examined, but the reduction of p-LAT demonstrates the inhibition of TCR activation. Next, flow cytometry further demonstrated that AX-024 significantly decreased IL-17 (a marker of proinflammation) and CD69 (a marker of T cell activation) expression in brain-infiltrating T cells at day 3 post-ICH (Fig. 2D-F), suggesting that early TCR activation inhibition can mitigate T cell activation in the brain post-ICH.

Inhibition of TCR activation by AX-024 prevents inflammatory response of brain-infiltrating T cells after ICH in mice

To investigate the effect of TCR inhibition on the T cells' inflammatory responses following ICH, flow cytometry was employed to profile T cell subsets in mice treated with or without AX-024. We found AX-024 significantly reduced the brain infiltration of both $CD4^+$ and $CD8^+$ T cells without affecting the number of T cell subsets in peripheral blood (Fig. 3A-B). Additionally, AX-024 decreased the production of pro-inflammatory cytokines (IFN-γ, IL-1β) but did not affect the anti-inflammatory cytokine IL-10 in $CD4^+$ T cells (Fig. 3C). Furthermore, AX-024 reduced the levels of cytolytic granules, Granzyme B and perforin, in $CD8^+$ T cells post-ICH (Fig. 3D).

Inhibition of TCR activation by AX-024 alleviates cerebral pro-inflammatory response after ICH in mice

We next tested whether inhibition of TCR activation could alter neuroinflammatory responses of brain inflammatory cells post-ICH. By counting cellular components in the ICH-affected brain, including microglia and brain-infiltrating leukocytes at day 3 post-ICH, we found that

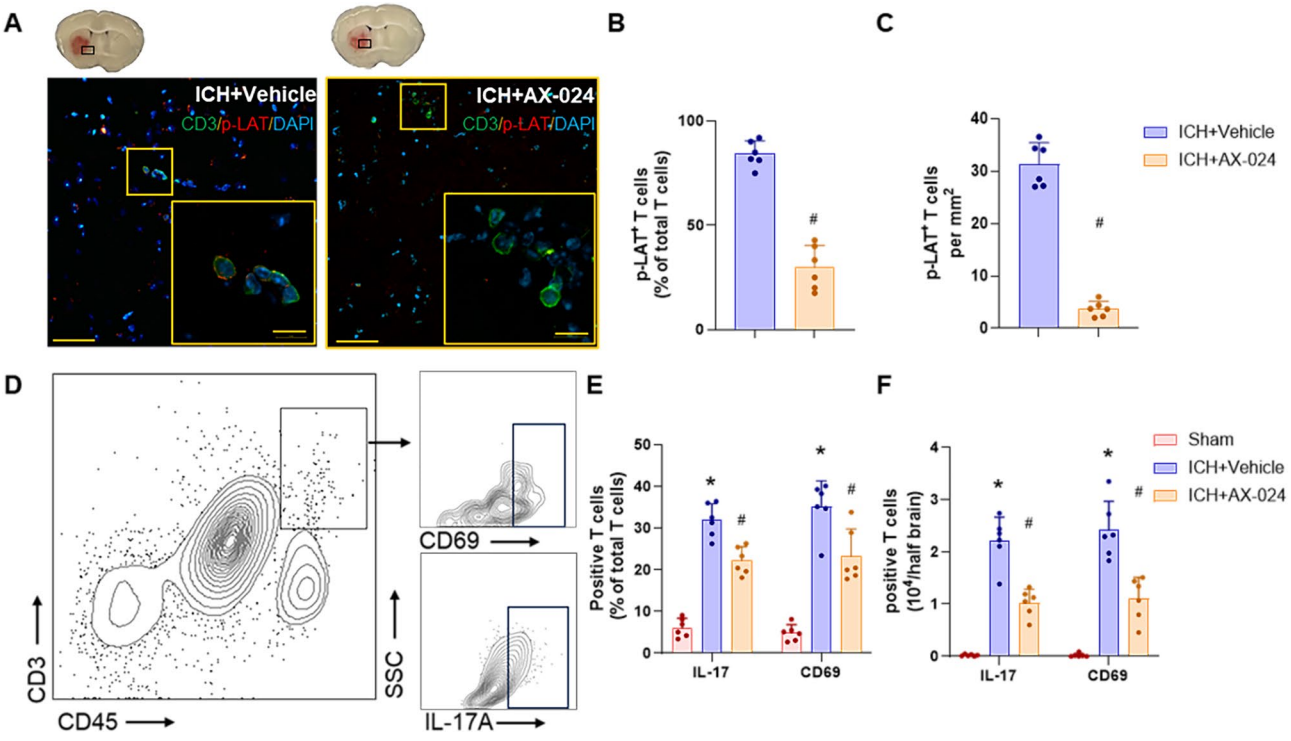

Fig. 2 Inhibition of TCR activation by AX-024 prevents brain-infiltrating T cell activation at acute phase after ICH in mice. ICH model was induced by collagenase IV injection in C57BL/6J mice. Brain tissue was obtained at 1 or 3 days after ICH. (**A**) Double immunostaining of TCR activation marker p-LAT with T cells ($CD3^+$) in the peri-hematoma region of ICH and ICH + AX-024 groups at 24 h post-ICH. Scale bar: 50 μm and (inset) 10 μm. (**B-C**) Comparison of the total T cell number, the percentage (**B**) and the cell count (**C**) of brain-infiltrating $CD3^+$ T cells expressing p-LAT in the peri-hematoma region at 24 h post-ICH. (**D**) Flow cytometry plots showing activated T cells (either IL-17 A or CD69 positive) in total brain-infiltrating T cells 3 days after ICH in sham, ICH and ICH + AX-024 groups. (**E-F**) Percentage (**E**) and the cell counts (**F**) of activated T cells (either IL-17 or CD69 positive) in total brain-infiltrating T cells at day 3 after ICH. $n = 6$ mice per group. Mean ± SD, $^*P < 0.05$ vs. Sham group, and $\#P < 0.05$ vs. ICH + Vehicle group. Student's t-test in **(B, C)** and two-way ANOVA in **(E, F)**

AX-024 administration (10 mg/kg, i.p.) at 1 h post-ICH led to a notable reduction in the counts of microglia and brain-infiltrating leukocytes, especially neutrophils and monocytes, during acute phase after ICH (Fig. 4B-C). We also measured the pro-inflammatory activation of microglia after ICH. The reduction of the pro-inflammatory activation marker caspase-1 by AX-024 administration suggests that AX-024 significantly attenuated microglial activation in the peri-hematoma region after ICH (microglia identified by the marker Iba1) (Fig. 4D-E). Furthermore, we tested the effects of AX-024 administration on inflammatory profiles of brain tissues after ICH. Using a cytokine array kit at 3 days post-ICH, our experimental results showed a shift toward a reduced inflammatory cytokine protein expression (CCL1, IFN-γ, IL-1α, IL-1β, IL-16, CXCL12) but elevated regulatory cytokine protein (C5/C5a, TREM-1) expressions in the ipsilateral brain tissues, compared to the vehicle-treated control mice (Fig. 4F). These results suggest that inhibition of TCR activation suppresses detrimental neuroinflammatory responses and restores inflammatory microenvironments of the brain tissue during the acute phase after ICH.

Validation of AX-024's specificity in inhibition of TCR activation in vitro

To validate the specificity of AX-024 in inhibition of TCR activation, we performed immune cell activation assays in vitro using isolated monocytes and T lymphocytes. Firstly, to determine whether AX-024 inhibits the inflammatory activation of non-T cell leukocytes, monocytes were isolated from naive C57BL/6J mice, cultured and stimulated with the damage-associated molecular pattern (DAMP), high mobility group box 1 (HMGB1) (500 ng/mL), a potent pro-inflammatory activator secreted from injured cells after ICH [29, 30] (Fig. 5A). After a 24-hour exposure with or without AX-024 (100 μM), RT-qPCR analysis showed that AX-024 exposure had no significant effects on HMGB1-stimulated increases of IL-1β and TNFα mRNA levels (Fig. 5B-C). However, the cytokine expression increases were significantly attenuated by TAK242 (an inhibitor of Toll-like receptor 4, 500 nM), as a positive control in cultured monocytes. Secondly, T lymphocytes were isolated from naive C57BL/6J mice and activated in vitro with a phorbol myristate acetate (PMA) and ionomycin cocktail to achieve TCR-independent stimulation or CD3/CD28 antibody-loaded

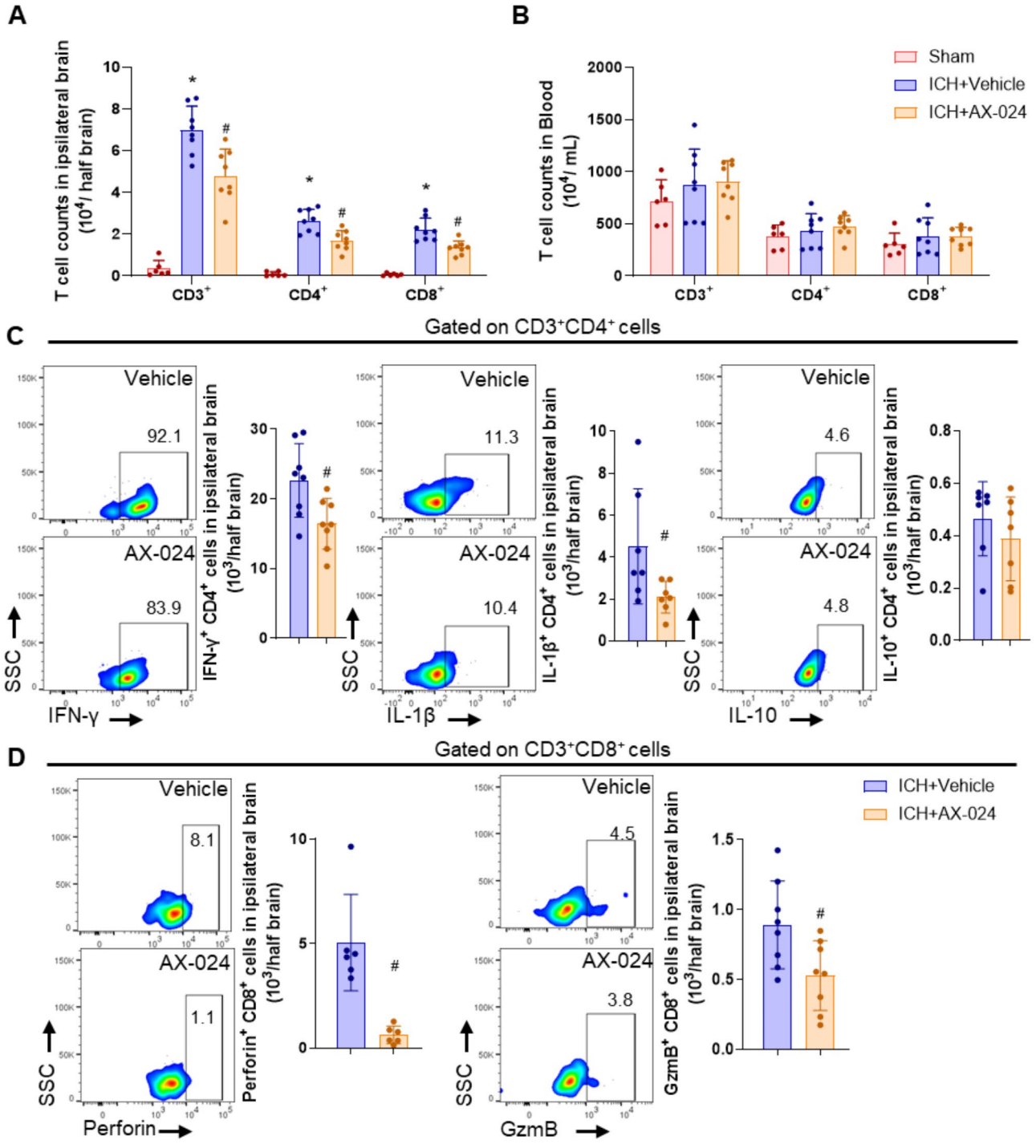

Fig. 3 Inhibition of TCR activation by AX-024 prevents inflammatory response of brain-infiltrating T cell after ICH in mice. ICH model was induced by collagenase IV injection in C57BL/6J mice. Brain tissue and peripheral blood were obtained at 3 days after ICH. (**A-B**) Flow cytometry analysis of T cells in brain (**A**) and peripheral blood (**B**) after ICH. The cell counts of $CD3^+$, $CD4^+$, and $CD8^+$ T cells in brain and blood was analyzed. (**C**) Flow cytometry analysis of cytokine IFN-γ, IL-1β, and IL-10 in brain-infiltrating $CD4^+$ T cell after ICH. (**D**) Flow cytometry analysis of perforin and granzyme B (GzmB) in brain-infiltrating $CD8^+$ T cell 3 days post-ICH. $n = 6–8$ mice per group. Mean ± SD, $^*P < 0.05$ vs. Sham group, and $\#P < 0.05$ vs. ICH + Vehicle group. Two-way ANOVA in (**A, B**) and Mann-Whitney U test in (**C, D**)

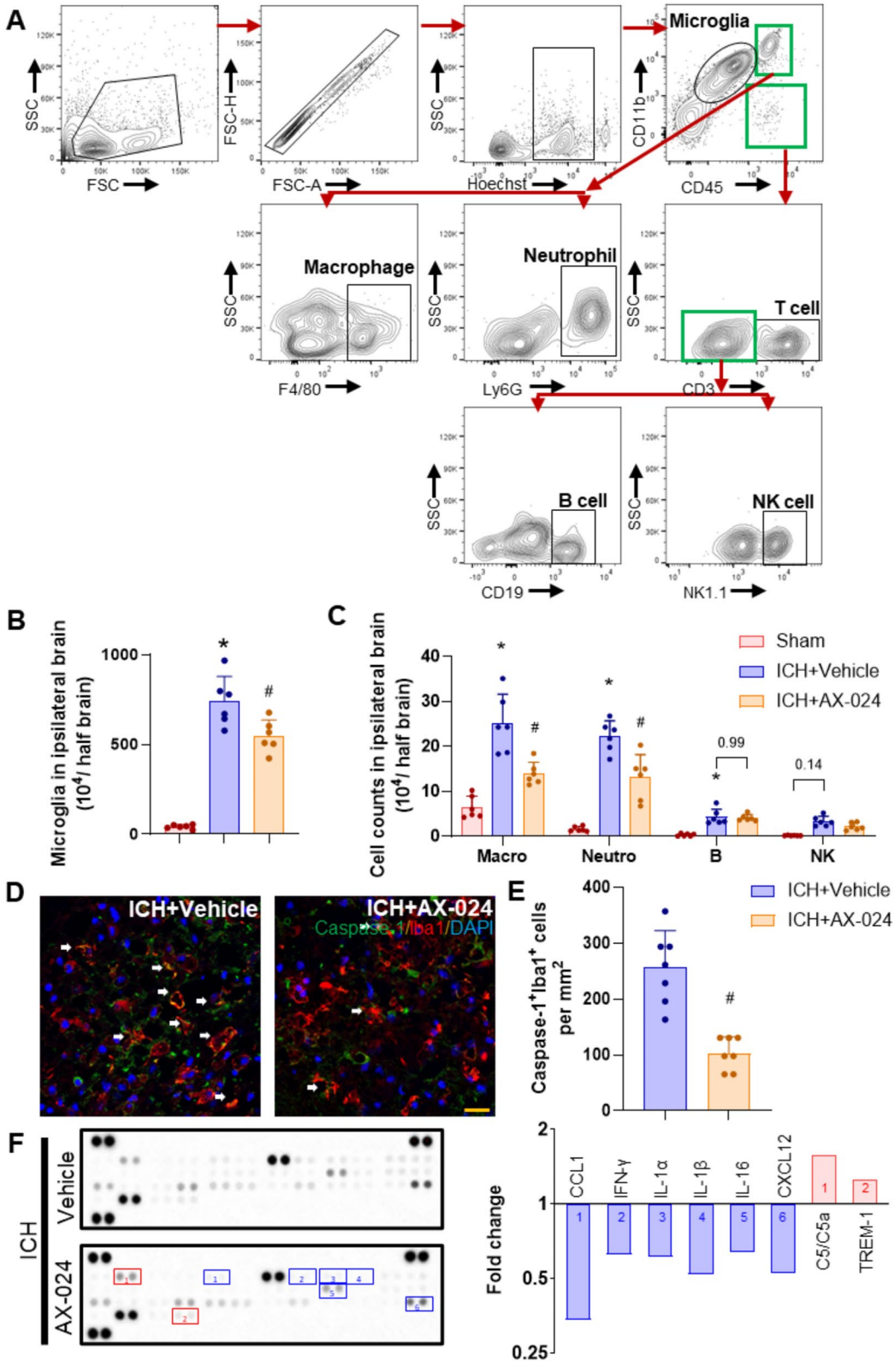

Fig. 4 (See legend on next page.)

(See figure on previous page.)

Fig. 4 Inhibition of TCR activation by AX-024 alleviates cerebral pro-inflammatory response after ICH in mice. ICH model was induced by collagenase IV injection in C57BL/6J mice. (**A**) Representative gating strategy for microglia and brain-infiltrating leukocytes. (**B-C**) Flow cytometry quantification showing cell counts of microglia (**B**), macrophages, neutrophils, B cells and NK cells (**C**) in sham, ICH, and ICH + AX-024 mice at 3 day after ICH. (**D-E**) Representative image (**D**) and quantification (**E**) of double staining of caspase-1 and Iba1 in peri-hematoma region at day 3 post ICH. Scale bar: 20 μm. White arrows: Caspase-1$^+$ microglia (Iba1$^+$). $n = 6$–8 mice per group. Mean ± SD, $^*P < 0.05$ vs. Sham group, and $\#P < 0.05$ vs. ICH + Vehicle group. (**F**) Cytokine array image and of ipsilateral brain tissue with or without AX-024 treatment. Quantification of cytokine fold change between ICH and ICH + AX-024 group, $n = 2$ independent experiments.; blue or red, cytokines fold change down- or up- regulated in AX-024 treated group, respectively. Mean. One-way ANOVA in (**B**), two-way ANOVA in (**C**), and student's T test in (**E**)

microbeads to achieve TCR-dependent stimulation (Fig. 5D). After 24 h of exposure, flow cytometry analysis demonstrated that AX-024 exposure markedly reduced TCR-dependent activation in T cells exposed to CD3/CD28 antibody-loaded microbeads, as evidenced by the reduction of IL-17 and CD69 expression elevation of T lymphocytes following CD3/CD28 induced TCR-dependent activation, but not following TCR-independent activation with PMA and ionomycin cocktail (Fig. 5E-F). These results validate the specificity of AX-024 for inhibiting TCR-dependent T cell activation.

Inhibition of TCR activation by AX-024 mitigates acute brain edema and improves neurological outcomes after ICH in mice

Next, we performed a series of experiments to evaluate the impact of TCR activation in acute brain damage and neurological deficits after ICH (Fig. 6A). Firstly, to evaluate the effects of TCR activation inhibition in acute brain damage, we measured brain edema (water content) at day 3 post-ICH. Our results showed AX-024 administration (10 mg/kg, i.p., initiated at 1 h after ICH) significantly reduced brain edema formation in the ipsilateral hemisphere compared to ICH controls (Fig. 6B). Next, we quantified a key brain tissue damage marker, white matter injury at 15 days following ICH after completion of neurobehavioral assessments, via a double staining for MBP and SMI32 (Fig. 6C-E). The demyelinating lesion volume and white matter injury was substantially lower in AX-024 treated ICH mice compared with vehicle treated ICH mice measured by the loss of MBP [31] andabnormal SMI32/MBP ratio [32], indicating a decreased white matter injury by AX-024 treatment. Lastly, we assessed the effects AX-024 administration in neurobehavioral deficits. Our experimental results showed AX-024 administration significantly improved sensorimotor function up to 14 days in mNSS, adhesive removal, and foot fault tests compared to mice receiving vehicle treatment (Fig. 6F-H). Moreover, the MWM test showed a significantly worse learning and spatial memory ability in ICH animals versus sham controls, and administration of AX-024 enhances the frequency of successful platform location within a certain time following ICH in mice (Fig. 6I-J). All these results suggest that inhibition of TCR activation by AX-024 administration significantly improves the sensorimotor function and cognitive function after ICH in mice, demonstrating that selectively targeting TCR activation by AX-024 administration can reduce acute brain damage, white matter injury and long-term neurological deficits after ICH.

Discussion

Our present study investigates early TCR activation of brain-infiltrating T cells in the acute phase of ICH. By using a pharmacological approach with AX-024, a specific inhibitor of TCR activation, we, for the first time, provided experimental evidence that TCR activation contributes to acute T cell activation in the brain after ICH, which accelerates the acute activation and recruitment of T cells, and other peripheral immune cells, and ultimately contributes to the brain edema, white matter injury, and neurological deficits following ICH. Our experimental findings strongly suggest that the early TCR-activation plays a crucial role in activating brain-infiltrating T lymphocytes and contributes to its detrimental roles in neuroinflammation-derived acute brain damage and neurological deficits. Thus, selectively inhibiting TCR activation of brain-infiltrating T lymphocytes may modulate neuroinflammation and improve neurological outcomes after ICH.

Although the process for TCR activation is dynamic and complex, it has been accepted that T cell activation is regulated by the TCR recognizing peptide antigens presented by major histocompatibility complex molecules. The intricate TCR complex, including TCRαβ or TCRγδ heterodimers along with the CD3 molecular assemblies, not only identifies antigens but also transduces antigen recognition signals intracellularly via tyrosine phosphorylation pathways involving kinases including LCK and LAT [33]. These signaling events facilitate the recruitment of ZAP70, amplifying the initial activation signal, leading to downstream pathways such as Ca^{2+} influx, LCK and LAT phosphorylation and Ras/Erk pathway activation and ultimately resulting in T cell proliferation, CD69 expression, and cytokine production and release [34]. In this study, we first confirmed the presence of TCR activation in brain parenchyma in the early stage following ICH using flow cytometry and immunofluorescence techniques. However, the underlying mechanisms of TCR activation in the brain require further investigation. Additionally, we cannot exclude the possibility that DAMPs, such as heat shock proteins, HMGB1, and

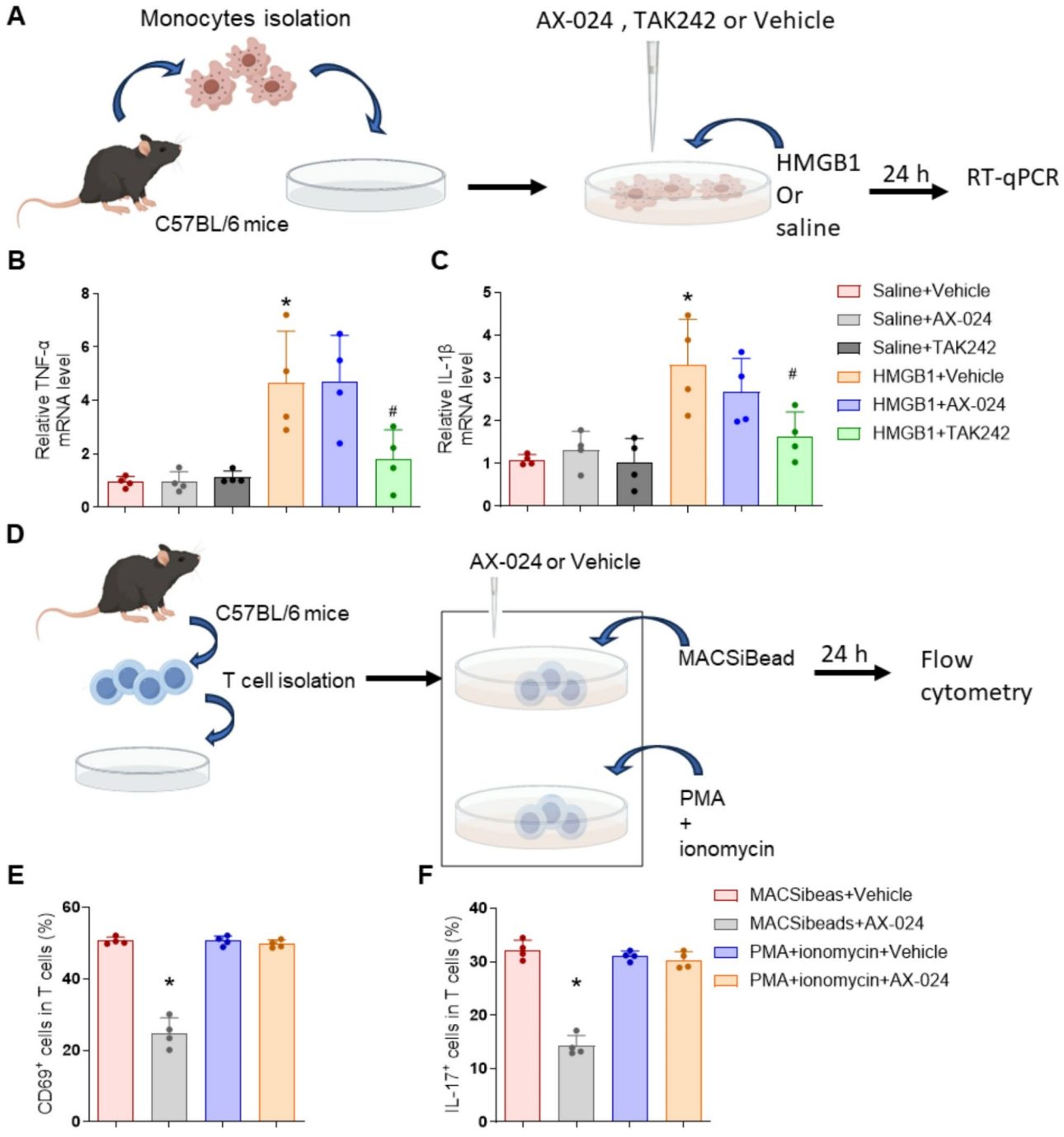

Fig. 5 Validation of AX-024's specificity in inhibition of TCR activation in vitro. (**A**) Monocytes were harvested from spleen and cultured with HMGB1 or control saline, followed by treatment with AX-024 or vehicle. (**B-C**) RT-qPCR analysis of mRNA levels showing expression of TNF-α (**B**) and IL-1β (**C**) in groups of monocytes receiving indicated treatment at 24 h. A total of 4 independent experiments were repeated, $n = 3$ mice per group/experiment. Mean ± SD. $^{*}P < 0.05$ vs. Saline + Vehicle, and $\#P < 0.05$ vs. HMGB1 + Vehicle. (**D**) Naïve T cells were negatively isolated from spleen and cultured with CD3/CD28-loaded MACSibeads or PMA + ionomycin, followed by treatment with AX-024 or vehicle. (**E-F**) Flow cytometry analysis of cytokine levels in cultured T cells showing expression of CD69 (**E**) and IL-17 (**F**) in groups of T cells receiving the indicated treatment at 24 h. A total of 4 independent experiments were repeated, $n = 3$ mice per group/experiment. Mean ± SD, $^{*}P < 0.05$ vs. MACSibeads + Vehicle group. One-way ANOVA in (**B, C, D, E**)

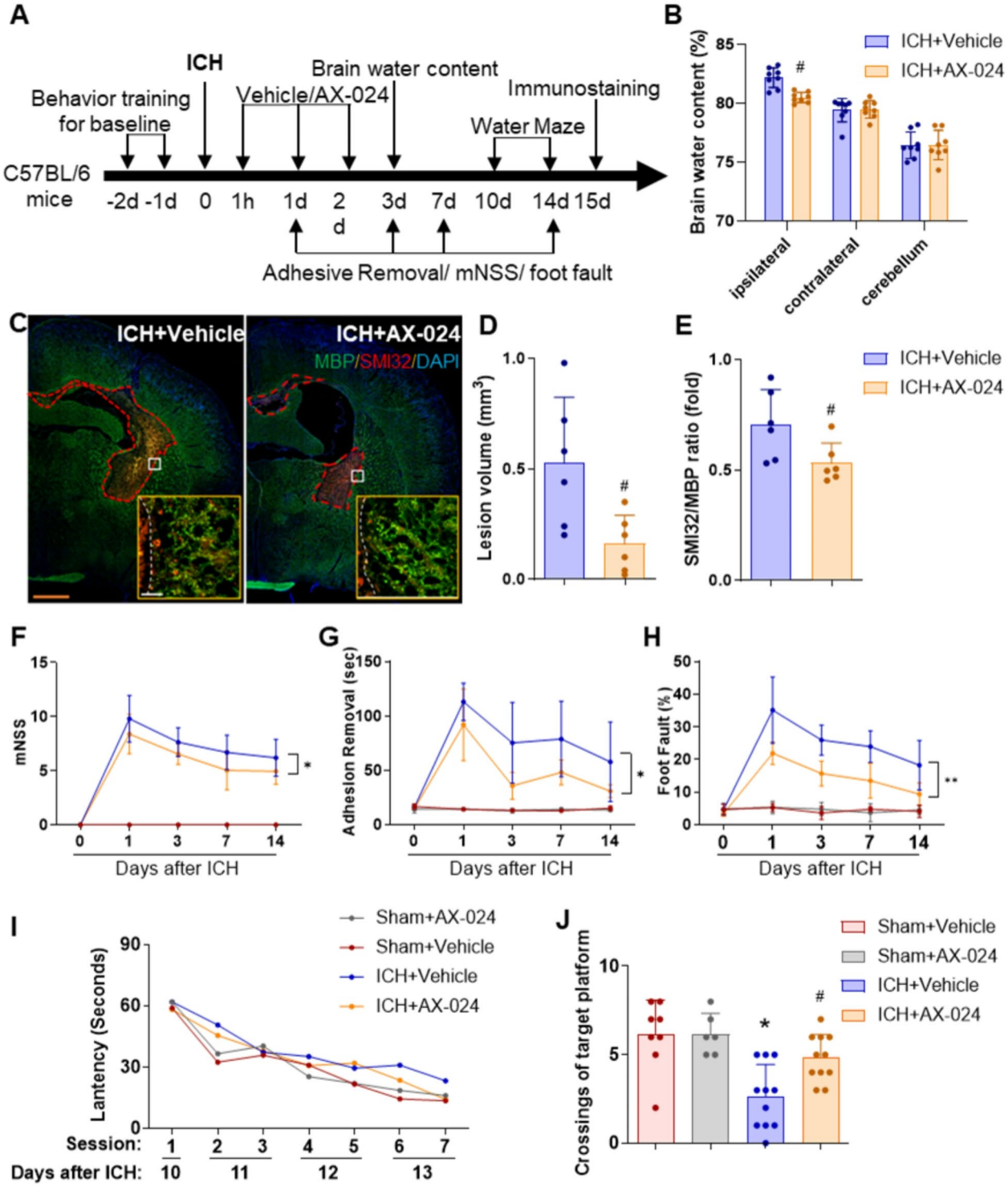

Fig. 6 Inhibition of TCR activation by AX-024 mitigates acute brain edema and improves neurological outcomes after ICH in mice. ICH model was induced by collagenase IV injection in C57BL/6J mice. (**A**) Schematic diagram showing the timeline of the experimental procedures for the pathological evaluation and neurobehavioral assessments. (**B**) Brain water content of ipsilateral hemisphere at 3 days after ICH. $n = 8$ mice per group, (**C-E**) Representative double-immunostaining images (**C**) of MBP (green) plus SMI32 (red) show the demyelinating lesion (dashed red circle) and quantification of demyelinating lesion volume (**D**) and SMI32/MBP ratio (**E**) in peri-lesion area at 15 days after ICH. Scale bar: 1 mm and (inset = 100 μm). $n = 6$ mice per group. (**F-J**). mNSS (**F**), adhesive removal test (**G**), foot fault test (**H**), and MWM (**I-J**) were performed to assess neurobehavioral outcomes up to 14 days after ICH. $n = 6$–12 mice per group. Mean ± SD.*$P < 0.05$ vs. Sham group, and #$P < 0.05$ vs. ICH + Vehicle group. Mann–Whitney U test in (**B**), student's T test in (**D, E**), two-way ANOVA in (**F, G, H, I**), and one-way ANOVA in (**J**)

adenosine, along with cytokines and coagulation factors, that are released from disrupted cellular components are recognized by specific receptors on immune cells, initiating an activation cascade [35] and causing T cell activation in a TCR-independent manner [36].

Studies have traditionally focused on the complex role of T cells in relation to inflammation, BBB disruption, neurotoxicity, and brain edema progression [4, 6, 37–40]. However, the exact contributions of antigen-specific T cells to damage post-brain injury are still under investigation [16]. Therefore, to elucidate the role of TCR-dependent/antigen-specific T-cell activation during the acute phase of ICH and to define the causal roles of TCR activation in brain pathological evolution during the acute phase after ICH, we applied a specific TCR activation inhibitor AX-024 to test our hypothesis. AX-024 is a small molecule with a molecular weight of 339.4 Da, characterized by its ability to traverse the BBB and penetrate the brain parenchyma [19]. It specifically binds to the Nck SH3.1 domain in T cells, inhibiting NCK-CD3 interactions [41]. Previous studies have suggested that AX-024 can mitigate the intensity of inflammation in various experimental models, including psoriasis, anemia, and the experimental autoimmune encephalomyelitis (EAE) model of MS [19]. We administered AX-024 10 mg/kg daily according to the established dose regimen from previously published experiments [19]. Considering the first three days constitute the critical phase of T cell infiltration into the brain following ICH, the delivery of AX-024 was confined up to 3 days after ICH [4, 11]. In this study, we further validated the specificity of AX-024 in inhibiting TCR activation following ICH. Our results showed that AX-024 only inhibits TCR-dependent activation and not TCR-independent mechanisms, and also does not inhibit the activation of monocytes, which is consistent with other early studies [19, 41].

By inhibiting TCR activation with AX-024, we found a consequent reduction of brain-infiltrating T lymphocyte count and their activation. Furthermore, since T cells are principal cytokine-secreting cells, we investigated the inflammatory phenotypes of brain-infiltrating T cells post-ICH. Our results showed AX-024 administration reduced expression levels of pro-inflammatory cytokines but not anti-inflammatory cytokines in brain-infiltrating $CD4^+$ T cells. Furthermore, AX-024 reduced the levels of cytolytic granules, Granzyme B and perforin, in $CD8^+$ T cells in the acute phase post-ICH, suggesting that AX-024 selectively attenuates the pro-inflammatory and cytotoxic activities of T cells, potentially mitigating T cell-mediated damage while preserving regulatory functions that may aid in recovery. Interestingly, a previous study has reported that inhibiting or reducing the intensity of TCR activation can decrease the differentiation of pro-inflammatory Th1/Th17 cells while increasing the differentiation of anti-inflammatory Th2/Treg cells in EAE model [19], and these suggest that TCR activation may be involved in directing the differentiation of naive T cells [42].

To investigate the regulatory role of T cells in neuroinflammation within the brain, we conducted flow cytometry to assess the infiltration of inflammatory cells. Our findings indicate that inhibiting TCR activation with AX-024 reduces cellular counts of microglia, and brain infiltration of monocytes/macrophages, and neutrophils. Furthermore, following AX-024 administration, the inflammatory activation of microglia was also diminished, and the overall expression of inflammatory cytokines in the brain was decreased. These findings underscore that T cells play a complex role in CNS inflammation, not only by directly infiltrating into brain but also by regulating the activity of resident immune cells, such as microglia [43, 44], and influencing the broader immune response [45]. By inhibiting TCR activation, AX-024 appears to suppress the immune cascade that leads to both cellular infiltration and inflammatory activation in the brain.

It has been well demonstrated that brain edema is a quantifiable marker of secondary brain damage after ICH and is associated with a poor prognosis [46]. Our previous study reported that brain-infiltrating T cells can exacerbate acute peri-hematoma edema formation by triggering endothelial cell death and compromising BBB integrity [11]. One more brain injury marker is white matter injury following ICH, which is especially impactful for recovery after ICH, because of the white matter's central role in neural communication, its vulnerability to inflammation and oxidative stress-associated secondary injury, limited regenerative ability, and importance for cognitive and motor functions [47, 48]. Importantly, neurological outcomes are essential for evaluating the effectiveness of new therapeutic interventions for ICH, because they directly measure how effectively a treatment restores function and may predict long-term recovery [47]. Excitingly, our experimental results showed that AX-024 administration significantly reduced cerebral edema and white matter injury following ICH. Furthermore, we also demonstrated AX-024 can improve sensorimotor function and cognitive function after ICH. Together, these experimental results suggest that selectively inhibiting TCR activation may be a promising immunoregulatory strategy for protecting against pro-inflammation-associated secondary brain damage and reducing neurological deficits after ICH.

We recognize that this study has several limitations. First, we did not identify APCs or specific antigens involved in T cell activation post-ICH. Future studies should assess MHC expression to postulate potential APCs and employ tetramer staining to pinpoint the

antigens that activate brain-infiltrating T cells [49]. Second, our exclusive use of male mice does not address potential sex differences in ICH outcomes, so the impact of TCR signaling inhibition in female mice remains an open area for further inquiry [50]. Third, we did not elucidate the underlying molecular mechanisms of TCR activation-derived detrimental neuroinflammation response and consequent neurovascular pathology following ICH, which will be carefully investigated in the near future. Fourth, we did not fully evaluate the therapeutic potential of AX-024 in this study, but only provided experimental evidence as a proof-of-concept investigation. The translational potential of AX-024 for clinical care needs to be fully investigated in the future. Fifth, despite significant attenuation of TCR activation by AX-024 administration, we observed a portion of brain-infiltrating T cells continued to activate, indicating possible TCR-independent activation pathways involved following ICH, which warrants further investigation. Sixth, this study was primarily focused on the activation of TCR in brain-infiltrated T cells because our previous study performed dynamic tracking of T cell activation via genetically edited calcium influx, which identified not the circulating T lymphocytes but the brain-infiltrating T lymphocytes were activated following ICH [11]. Moving forward, studies are needed to further explore the impact of TCR activation on peripheral inflammation post-ICH, including more granular experiments to comprehensively understand TCR activation across different T cell subsets post-ICH. Lastly, TCR co-signaling receptors are crucial components of TCR-dependent T cell activation [51], but this aspect was not explored in our current study, which requires investigation in the future.

In conclusion, our present study demonstrates an early TCR activation of brain-infiltrating T lymphocytes, which contributes to the pro-inflammatory activation of T lymphocytes, results in amplifying neuroinflammation, and ultimately exacerbates brain damage. Specific inhibition of TCR activation with AX-024 administration reduces T cell activation and subsequent detrimental effects in terms of neuroinflammation, acute brain damage, and neurological deficits following ICH. However, the detailed underlying molecular mechanisms need to be fully elucidated. The translational potential of AX-024 and other pharmacologic interventions that target TCR activation for treating ICH warrants more comprehensive investigation in the future.

Author contributions

X.W., A. D. and Q.L. formulated the concept and designed the studies. Y.X., Y.W., T.Y.S, M.S, D.X., N.L., Y.J., M.K., N.W. performed the experiments and analyzed the results. Y.X., W.-N.J., P.K., F.-D.S., and X.W. interpreted the results and drafted the manuscript.

Funding

This research was supported by Tulane Research Centers of Excellence Awards and the National Institutes of Health Grants NS114286 (to P.K.) and AG074489 (to P.K.).

Data availability

The datasets used and/or analysed during the current study are available from the corresponding author on reasonable request.

Declarations

Ethics approval

All animal experiments were performed with ethics approval (protocol ID: 2118) from the Institutional Animal Care and Use Committee (IACUC) of Tulane University.

Competing interests

The authors declare no competing interests.

Received: 3 January 2025 / Accepted: 25 February 2025
Published online: 13 March 2025

References

1. Sun Q, et al. Neurovascular units and Neural-Glia networks in intracerebral hemorrhage: from mechanisms to translation. Transl Stroke Res. 2021;12(3):447–60.
2. Hemphill JC 3, et al. Guidelines for the management of spontaneous intracerebral hemorrhage: A guideline for healthcare professionals from the American heart association/american stroke association. Stroke. 2015;46(7):2032–60.
3. Alsbrook DL, et al. Neuroinflammation in acute ischemic and hemorrhagic stroke. Curr Neurol Neurosci Rep. 2023;23(8):407–31.
4. Mracsko E, et al. Leukocyte invasion of the brain after experimental intracerebral hemorrhage in mice. Stroke. 2014;45(7):2107–14.
5. Zhang P, et al. Single-cell RNA sequencing reveals the evolution of the immune landscape during perihematomal edema progression after intracerebral hemorrhage. J Neuroinflammation. 2024;21(1):140.
6. Rolland WB, et al. Fingolimod reduces cerebral lymphocyte infiltration in experimental models of rodent intracerebral hemorrhage. Exp Neurol. 2013;241:45–55.
7. Li YJ, et al. Fingolimod alters inflammatory mediators and vascular permeability in intracerebral hemorrhage. Neurosci Bull. 2015;31(6):755–62.
8. Sun N, et al. Selective Sphingosine-1-Phosphate receptor 1 modulation attenuates experimental intracerebral hemorrhage. Stroke. 2016;47(7):1899–906.
9. Cohen JA, Chun J. Mechanisms of Fingolimod's efficacy and adverse effects in multiple sclerosis. Ann Neurol. 2011;69(5):759–77.
10. Xue M, Yong VW. Neuroinflammation in intracerebral haemorrhage: immunotherapies with potential for translation. Lancet Neurol. 2020;19(12):1023–32.
11. Shi SX, et al. CD4(+) T cells aggravate hemorrhagic brain injury. Sci Adv. 2023;9(23):eabq0712.
12. Li MO, Rudensky AY. T cell receptor signalling in the control of regulatory T cell differentiation and function. Nat Rev Immunol. 2016;16(4):220–33.
13. Ohno H, et al. CD2 can mediate TCR/CD3-independent T cell activation. J Immunol. 1991;146(11):3742–6.
14. Oberg HH, et al. Regulation of T cell activation by TLR ligands. Eur J Cell Biol. 2011;90(6–7):582–92.
15. Shi SX et al. T-Lymphocyte interactions with the neurovascular unit: implications in intracerebral hemorrhage. Cells. 2022;11(13).
16. Durocher M, et al. Molecular correlates of hemorrhage and edema volumes following human intracerebral hemorrhage implicate inflammation, autophagy, mRNA splicing, and T cell receptor signaling. Transl Stroke Res. 2021;12(5):754–77.
17. Schulze J, et al. Central nervous System-Infiltrating T lymphocytes in stroke are activated via their TCR (T-Cell Receptor) but lack CD25 expression. Stroke. 2021;52(9):2939–47.
18. Puy L, et al. Intracerebral haemorrhage. Nat Rev Dis Primers. 2023;9(1):14.
19. Borroto A, et al. First-in-class inhibitor of the T cell receptor for the treatment of autoimmune diseases. Sci Transl Med. 2016;8(370):370ra184.

20. Li M, et al. Colony stimulating factor 1 receptor Inhibition eliminates microglia and attenuates brain injury after intracerebral hemorrhage. J Cereb Blood Flow Metab. 2017;37(7):2383–95.
21. Jiang Y, et al. Endocrine regulator rFGF21 (Recombinant human fibroblast growth factor 21) improves neurological outcomes following focal ischemic stroke of type 2 diabetes mellitus male mice. Stroke. 2018;49(12):3039–49.
22. Bouet V, et al. The adhesive removal test: a sensitive method to assess sensorimotor deficits in mice. Nat Protoc. 2009;4(10):1560–4.
23. Choi YK, et al. Dual effects of carbon monoxide on pericytes and neurogenesis in traumatic brain injury. Nat Med. 2016;22(11):1335–41.
24. Sirbulescu RF, et al. Intraparenchymal application of mature B lymphocytes improves structural and functional outcome after contusion traumatic brain injury. J Neurotrauma. 2019;36(17):2579–89.
25. Shi SX, et al. IL (Interleukin)-15 bridges Astrocyte-Microglia crosstalk and exacerbates brain injury following intracerebral hemorrhage. Stroke. 2020;51(3):967–74.
26. Gan Y, et al. Ischemic neurons recruit natural killer cells that accelerate brain infarction. Proc Natl Acad Sci U S A. 2014;111(7):2704–9.
27. Liu N et al. Annexin A2 deficiency exacerbates neuroinflammation and Long-Term neurological deficits after traumatic brain injury in mice. Int J Mol Sci. 2019;20(24).
28. Cheng N, et al. Brain-derived programmed death-ligand 1 mediates immunosuppression post intracerebral hemorrhage. J Cereb Blood Flow Metab. 2022;42(11):2048–57.
29. Lei C, et al. Activation of the high-mobility group box 1 protein-receptor for advanced glycation end-products signaling pathway in rats during neurogenesis after intracerebral hemorrhage. Stroke. 2015;46(2):500–6.
30. Shikata E, et al. An imbalance between RAGE/MR/HMGB1 and ATP1alpha3 is associated with inflammatory changes in rat brain harboring cerebral aneurysms prone to rupture. J Neuroinflammation. 2022;19(1):161.
31. Zheng J, et al. Temporal dynamics of microglia-astrocyte interaction in neuroprotective glial Scar formation after intracerebral hemorrhage. J Pharm Anal. 2023;13(8):862–79.
32. Yao M, et al. Modulation of the proteoglycan receptor PTPsigma promotes white matter integrity and functional recovery after intracerebral hemorrhage stroke in mice. J Neuroinflammation. 2022;19(1):207.
33. Alcover A, Alarcon B, Bartolo VD. Cell biology of T cell receptor expression and regulation. Annu Rev Immunol. 2018;36:103–25.
34. Shah K, et al. T cell receptor (TCR) signaling in health and disease. Signal Transduct Target Ther. 2021;6(1):412.
35. Shi K, et al. Global brain inflammation in stroke. Lancet Neurol. 2019;18(11):1058–66.
36. Derkow K, et al. Microglia induce neurotoxic IL-17 + gammadelta T cells dependent on TLR2, TLR4, and TLR9 activation. PLoS ONE. 2015;10(8):e0135898.
37. Komai-Koma M, et al. TLR2 is expressed on activated T cells as a costimulatory receptor. Proc Natl Acad Sci U S A. 2004;101(9):3029–34.
38. Kebir H, et al. Human TH17 lymphocytes promote blood-brain barrier disruption and central nervous system inflammation. Nat Med. 2007;13(10):1173–5.
39. Loftspring MC, et al. Intracerebral hemorrhage leads to infiltration of several leukocyte populations with concomitant pathophysiological changes. J Cereb Blood Flow Metab. 2009;29(1):137–43.
40. Xin L, et al. Commensal microbes drive intestinal inflammation by IL-17-producing CD4 + T cells through ICOSL and OX40L costimulation in the absence of B7-1 and B7-2. Proc Natl Acad Sci U S A. 2014;111(29):10672–7.
41. Alarcon B, Borroto A. Small molecule AX-024 targets T cell receptor signaling by disrupting CD3epsilon-Nck interaction. J Biol Chem. 2020;295(29):10076.
42. Gaud G, Lesourne R, Love PE. Regulatory mechanisms in T cell receptor signalling. Nat Rev Immunol. 2018;18(8):485–97.
43. Shi L, et al. Treg cell-derived osteopontin promotes microglia-mediated white matter repair after ischemic stroke. Immunity. 2021;54(7):1527–e15428.
44. Zheng Y, et al. T cell interactions with microglia in immune-inflammatory processes of ischemic stroke. Neural Regen Res. 2025;20(5):1277–92.
45. Zhou S, et al. CCL5 mediated astrocyte-T cell interaction disrupts blood-brain barrier in mice after hemorrhagic stroke. J Cereb Blood Flow Metab. 2024;44(3):367–83.
46. Chen Y, et al. Perihematomal edema after intracerebral hemorrhage: an update on pathogenesis, risk factors, and therapeutic advances. Front Immunol. 2021;12:740632.
47. Magid-Bernstein J, et al. Cerebral hemorrhage: pathophysiology, treatment, and future directions. Circ Res. 2022;130(8):1204–29.
48. Xiao L, et al. Secondary white matter injury mediated by neuroinflammation after intracerebral hemorrhage and promising therapeutic strategies of targeting the NLRP3 inflammasome. Curr Neuropharmacol. 2023;21(3):669–86.
49. Klenerman P, Cerundolo V, Dunbar PR. Tracking T cells with tetramers: new Tales from new tools. Nat Rev Immunol. 2002;2(4):263–72.
50. Umeano O, et al. Gender and age interact to affect early outcome after intracerebral hemorrhage. PLoS ONE. 2013;8(11):e81664.
51. Liu Y, et al. T-cell receptor signaling modulated by the co-receptors: potential targets for stroke treatment. Pharmacol Res. 2023;192:106797.

Publisher's note